Article

Geochemical Characterization and Heavy Metal Sources in PM$_{10}$ in Arequipa, Peru

Jianghanyang Li [1,*], **Greg Michalski** [1,2], **Elizabeth Joy Olson** [1], **Lisa R. Welp** [1], **Adriana E. Larrea Valdivia** [3,4], **Juan Reyes Larico** [3,4], **Francisco Alejo Zapata** [3,4] **and Lino Morales Paredes** [3,4]

1   Department of Earth, Atmospheric, and Planetary Sciences, Purdue University, West Lafayette, IN 47907, USA; gmichals@purdue.edu (G.M.); ejolson@purdue.edu (E.J.O.); lwelp@purdue.edu (L.R.W.)
2   Department of Chemistry, Purdue University, West Lafayette, IN 47907, USA
3   Centro de Investigacion de Contaminantes Ambientales, Laboratorio LABINVSERV del Departamento de Química, Universidad Nacional de San Augustín de Arequipa, Arequipa 04001, Peru; alarrea@unsa.edu.pe (A.E.L.V.); jreyesl@unsa.edu.pe (J.R.L.); falejo@unsa.edu.pe (F.A.Z.); lmoralesp@unsa.edu.pe (L.M.P.)
4   Environmental Pollutants Research Center and LABINVSERV Laboratory of Chemistry Department, Universidad Nacional de San Agustin de Arequipa, Arequipa 04001, Peru
*   Correspondence: li2502@purdue.edu

Abstract: Particulate matter smaller than 10 μm (PM$_{10}$) is an important air pollutant that adversely affects human health by increasing the risk of respiratory and cardiovascular diseases. Recent studies reported multiple extreme PM$_{10}$ levels at high altitude Peruvian cities, which resulted from a combination of high emissions and limited atmospheric circulation at high altitude. However, the emission sources of the PM$_{10}$ still remain unclear. In this study, we collected PM$_{10}$ samples from four sites (one industrial site, one urban site, and two rural sites) at the city of Arequipa, Peru, during the period of February 2018 to December 2018. To identify the origins of PM$_{10}$ at each site and the spatial distribution of PM$_{10}$ emission sources, we analyzed major and trace element concentrations of the PM$_{10}$. Of the observed daily PM$_{10}$ concentrations at Arequipa during our sampling period, 91% exceeded the World Health Organization (WHO) 24-h mean PM$_{10}$ guideline value, suggesting the elevated PM$_{10}$ strongly affected the air quality at Arequipa. The concentrations of major elements, Na, K, Mg, Ca, Fe, and Al, were high and showed little variation, suggesting that mineral dust was a major component of the PM$_{10}$ at all the sites. Some trace elements, such as Mn and Mo, originated from the mineral dust, while other trace elements, including Pb, Sr, Cu, Ba, Ni, As and V, were from additional anthropogenic sources. The industrial activities at Rio Seco, the industrial site, contributed to significant Pb, Cu, and possibly Sr emissions. At two rural sites, Tingo Grande and Yarabamba, strong Cu emissions were observed, which were likely associated with mining activities. Ni, V, and As were attributed to fossil fuel combustion emissions, which were strongest at the Avenida Independencia urban site. Elevated Ba and Cu concentrations were also observed at the urban site, which were likely caused by heavy traffic in the city and vehicle brake wear emissions.

Keywords: PM$_{10}$; trace metals; metal emissions

1. Introduction

Particulate matter (PM) caused by traffic congestion and industrialization is one of the most important air pollutants in urban areas. Particles less than 10 μm in diameter (PM$_{10}$) adversely affect human health, especially in elderly and infant populations, by increasing the risk of respiratory and cardiovascular diseases [1,2]. Additionally, PM$_{10}$ can act as a carrier of toxic chemicals, such as aromatic compounds or heavy metals [3,4], further increasing their health risks. Therefore, elevated levels of PM$_{10}$ have become a growing concern, especially in developing countries [5,6]. PM$_{10}$ is a mixture of various materials,

such as organic/elemental carbon, inorganic ions, soil particles, and trace metals [7]. The origins of PM_{10} can be complicated, including multiple natural and anthropogenic sources. PM_{10} concentrations and its chemical composition usually display strong spatial and temporal variations that have been linked to changes in PM sources and/or gas-to-particle conversion chemistry [8–10]. Thus, understanding the chemical origins of PM_{10} and its variation is a useful tool to begin to control the PM_{10} level in polluted regions.

The chemical composition of PM_{10}, especially trace metal content, has been widely used to infer PM_{10} sources [11–14]. For example, elevated levels of Zn, Mn, As, Cr, and Cu have been found near industrial centers [15], and high levels of Pb, Fe, Cu, Zn, Ni, Cd, and Ba were found in PM_{10} derived from vehicle emissions [16,17]. PM_{10} originating from mining activities has been shown to display various geochemical signatures depending on the minerals mined. For example, elevated amounts of As and Sb were observed near gold mine tailings in Spain [18] and PM_{10} near two coal mine sites contained high level of As, Be, Cd, Cr, Co, Ni, and Pb [19]. Since the concentrations of trace metals in PM_{10} imprint the signals from their sources, analyzing the spatial and temporal variations of PM_{10} trace metal concentrations can help us identify the contributions of different PM_{10} sources.

There are relatively few studies on PM matter in many South American countries, including Peru. Those few studies investigating air quality in Peru have found extreme cases of air pollution due to limited atmospheric circulation in high altitude cities, lack of government oversight on large emission sources such as factories, and the prevalence of older vehicles still in use in many regions [6,20]. The city of Arequipa is an important industrial and commercial center of Peru with over 1 million residents. Anthropogenic emissions related to heavy traffic, industry, mining operations, and other activities were suggested to strongly affect Arequipa's air quality [21]. Furthermore, sparse precipitation, with mean annual precipitation of ~100 mm, limits wet removal of atmospheric PM thus increasing its residence time. A recent study [21] showed PM_{10} concentrations in Arequipa exceeded the 24-h air quality standard (50 µg/m^3), established by both the World Health Organization (WHO) and the Peruvian government, 75% of the time. The annual average PM_{10} concentrations at industrial and residential areas of Arequipa were measured to be 167 ± 40 µg/m^3 and 116 ± 41 µg/m^3, respectively, suggesting pervasive PM pollution. However, the relative importance of various emission sources leading to the observed high PM_{10} concentrations are unclear. Additionally, while four sampling sites at Arequipa displayed significant spatial variations in PM_{10} concentrations, it is unknown which sources are responsible for these spatial variations. Constraining the sources and spatial variations of the PM_{10} across the city of Arequipa can help us better understand the origins of air pollution in this region. In this study, we (1) identify the major emission sources of PM_{10} and trace metals, and (2) investigate the spatial variations of the PM_{10} sources among the four sites, by analyzing the geochemical characteristics and trace metal (Pb, Cu, Sr, Ba, V, Ni, As, and Th) concentrations of PM_{10} collected at four sites in Arequipa, Peru.

2. Methods

Four sites around the city of Arequipa were selected in our study: Rio Seco, Av. Independencia, Tingo Grande, and Yarabamba (Figure 1). The Rio Seco industrial site (altitude: 2490 m above sea level) is located to the north of the city of Arequipa and is the industrial district of the city including, among others, leather tanning, borate manufacturing, and brick production facilities. The roads in the Rio Seco district are mainly unpaved dirt, and the site is close to the entrance/exit of a major highway. The Av. Independencia urban site (altitude: 2414 m above sea level) is located in the downtown center of the city where both population density and vehicle traffic are high. The Tingo Grande site (altitude: 2197 m above sea level) is located at the rural region to the west of Arequipa. This site is 6 km away from a large, active open pit mine site where copper and manganese are mined. Yarabamba rural site (altitude: 2500 m above sea level) is located 9 km to the east of the mine site and 15 km from the city center.
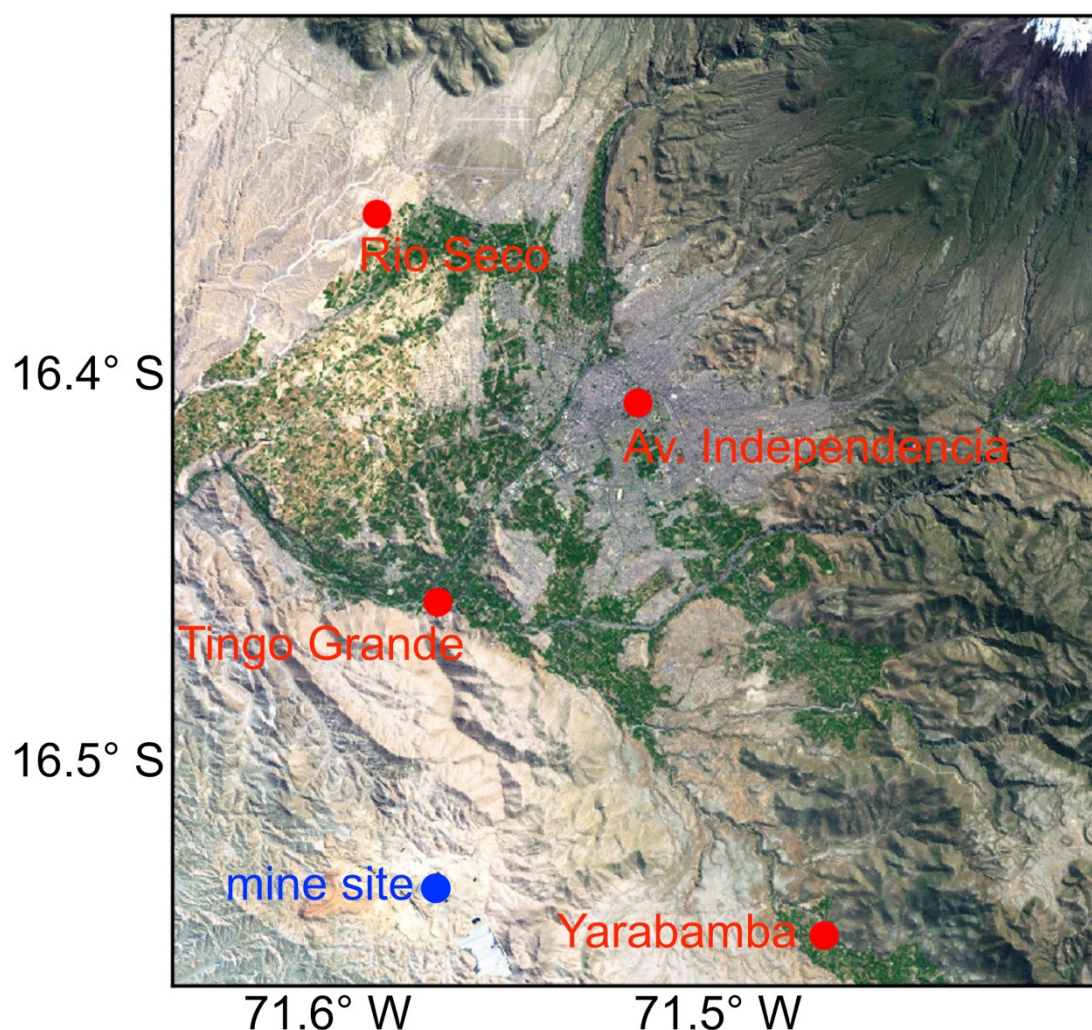
Figure 1. Map of the sampling sites. Industrial site (Rio Seco), urban site (Av. Independencia), and suburban sites (Tingo Grande and Yarabamba). Urban land cover appears grey in this image.

Daily PM_{10} samples were collected at these four sites from 6 February 2018, to 11 December 2018, using a high-volume PM_{10} aerosol sampler (HI-vol 3000, Ecotech). At each site, sampling was conducted for three consecutive days to collect three 24-h PM_{10} samples before moving to next site. PM_{10} was collected using pre-weighed, pre-combusted (200 °C for 4 h), quartz fiber filters (20.3 cm by 25.4 cm, Whatman-UK) at a flow rate of 1.13 m^3/min. After collection, the PM_{10} filters were reweighed to determine PM mass by difference using an analytical balance (Mettler Toledo, Columbus, OH, USA, XSE205DU), sliced into 10 equal length sections for use in various chemical analyses, and carefully preserved in paper envelopes to avoid post-sampling contamination. Trace metals were extracted using one of the filter sections following the protocols in US EPA Compendium Method IO-3.5 [22]. First, the filter was placed in a clean, 50 mL microwavable vessel. Then, 20 mL of acid solution (1.3 M ultrapure HNO_3 and 2 M ultrapure HCl dissolved in deionized water) was added into the vessel, ensuring the filter was completely submerged in the solution. Next, the solutions were placed in a microwave digester and heated at 170 °C for 23 min to dissolve all the water-soluble ions, surface absorbed ions, carbonates, and oxides. After the digestion, the extract was filtered through a 0.45 μm filter to remove undissolved residue. The solutions were then diluted using deionized water into 50 mL and the ion concentrations were measured using an ICP-MS (NexION 2000, PerkinElmer, Waltham, MA, USA). We analyzed one blank filter to determine the experimental blank, and the concentrations of major and trace elements (elements that are reported in this work) in

the blank sample were at least 1 order of magnitude lower than other samples. Replicated analysis showed that the standard errors for the element concentrations reported in this work are $\pm 10\%$. The analytical results were first used to calculate the air concentrations (in $\mu g/m^3$ for major elements and ng/m^3 for trace elements) of each element. Then, the mass-weighted concentrations were calculated using the air concentrations of each element and the PM_{10} concentration (in unit of % for major elements and ppm for trace elements).

3. Results and Discussions

3.1. PM_{10} and Major Element Concentrations

The study sites showed high PM_{10} concentrations during the sampling period and significant spatial variations among the four sites. The daily PM_{10} concentrations during the sampling period at all sites averaged at 97.7 ± 42.7 $\mu g/m^3$ (Figure 2, $n = 76$), which exceeded the WHO 24-h mean PM_{10} guideline value and national standard of 50 $\mu g/m^3$ by 195%. These results are consistent with annual monitoring of PM_{10} conducted by the Peru Ministry of Environmental Management office between 2007 and 2012, which found daily maximum PM_{10} concentration values frequently exceeded the WHO and national standard, reaching values as high as 342 $\mu g/m^3$, with an annual average of ~76 g/m^3 [23]. Our results are also similar to PM monitoring conducted by the mining company, which found that the annual average was 85.6 $\mu g/m^3$ during the period 2007–2013 [24], suggesting the PM_{10} level at Arequipa has been elevated in the past decade.
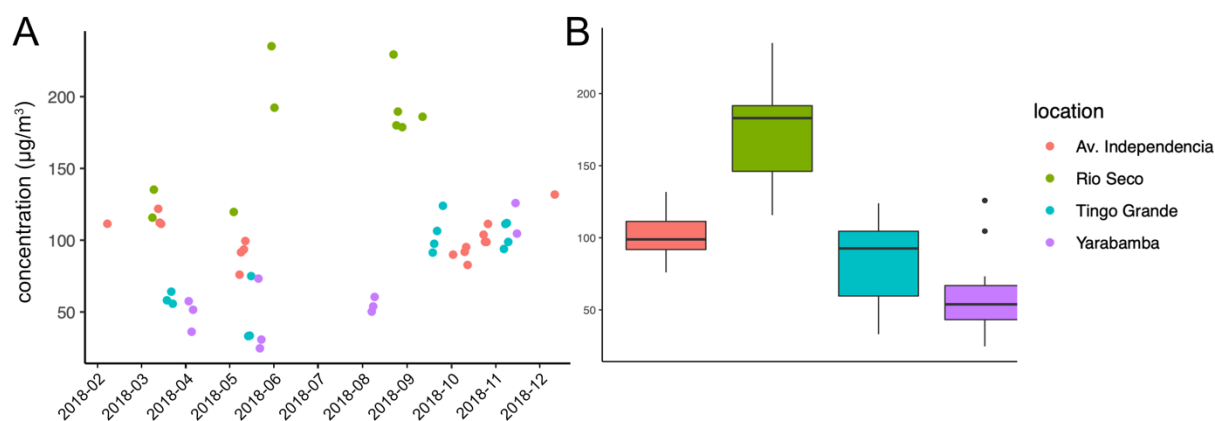

Figure 2. PM_{10} concentrations during the sampling period at all the sites. (**A**) Time series of observed PM_{10} concentrations in this study; (**B**) box plot of PM_{10} concentrations at each site.

PM_{10} concentrations did not display any obvious seasonal trends during the sampling period but showed significant spatial variations among the four sampling sites (Figure 2). Rio Seco had the highest daily PM_{10} concentrations, averaging 176.2 ± 41.3 $\mu g/m^3$ ($n = 10$), and Av. Independencia site had a lower average PM_{10} at 101.3 ± 14.1 $\mu g/m^3$ ($n = 17$), followed by Tingo Grande and Yarabamba at 82.5 ± 29.4 $\mu g/m^3$ ($n = 14$) and 60.8 ± 30.6 $\mu g/m^3$ ($n = 11$), respectively. The PM_{10} concentrations among different sites are statistically different, as the p-values between the PM_{10} concentrations of any two sites are less than 0.05. The strong spatial variations of PM_{10} concentrations among the four sites suggest a significant fraction of PM_{10} originates from local sources.

Our ICP-MS analysis showed that, on average, acid soluble Fe accounted for $1.0 \pm 0.4\%$ of PM_{10} mass, suggesting mineral dust was an important compound of the PM_{10} (Figure 3). Since we only measured the elemental concentrations in the non-silicate phase, the measured Fe should mainly exist as oxides (Fe_2O_3). Previous studies showed that Fe is a major element in mineral dust [25–27], and over half of Fe in mineral dust exists as iron oxides [28]. Mineral dust samples from the Saraha desert and the loess plateau in China contain 2.0–4.6% Fe; thus, the high Fe concentrations observed in our PM_{10} samples suggest that mineral dust is also a major component in Arequipa PM_{10}. The variation of Fe concentrations across the four sampling sites was small: the Fe concentrations at Rio Seco,

Av. Independencia, Tingo Grande, and Yarabamba averaged at $0.8 \pm 0.2\%$, $0.7 \pm 0.1\%$, $1.0 \pm 0.4\%$ and $1.3 \pm 0.7\%$, respectively, suggesting regional mineral dust contributed to the total PM_{10} mass similarly across the four sites.
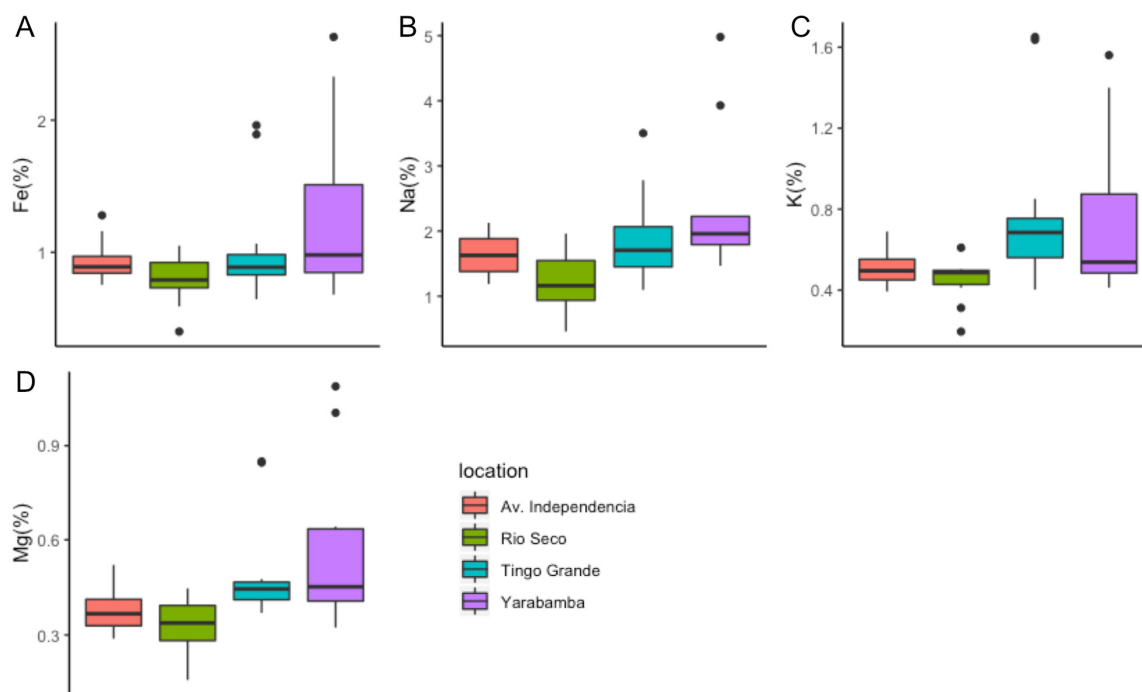

Figure 3. Box plot of major element concentrations (**A**: Fe, **B**: Na, **C**: K, **D**: Mg, in %) at each site.

The high concentrations of Na, K, and Mg in PM_{10} suggested inorganic salts were also a major component of the PM_{10} at these sites (Figure 3). The air concentrations of Na, K, and Mg in the PM_{10} samples averaged across all sites were 1.6 µg/m^3, 0.6 µg/m^3, 0.4 µg/m^3, and 1.3 µg/m^3, representing $1.8 \pm 0.7\%$, $0.6 \pm 0.3\%$, and $0.4 \pm 0.2\%$ of the PM_{10} mass, respectively. These elevated Na, K, and Mg concentrations were also observed in many arid regions such as the Atacama Desert, the Gobi Desert, and the Mojave Desert [25,29]. Additionally, these values were similar to the observed mass percentage of water-soluble Na ($1.4 \pm 0.7\%$), K ($0.7 \pm 0.5\%$) and Mg ($0.2 \pm 0.1\%$) concentrations in the $PM_{2.5}$ at Arequipa [30], indicating most of the observed Na, K, and Mg in the PM_{10} samples were in the form of water-soluble salts. The inorganic salts most likely originated from both the regional mineral dust and local surface soil. Surface soil in arid regions is usually enriched in inorganic salts. For example, a previous study at Pampas de La Joya, just 50 km southwest of Arequipa, observed significant amounts of halite (NaCl), gypsum ($CaSO_4 \cdot 2H_2O$), and calcite ($CaCO_3$) salts in surface soil [31,32]. Thus, we speculate soil entrainment at our sampling sites could also be an important source of Na, K, and Mg in our PM_{10} samples. Similar to Fe, concentrations of Na, K, and Mg did not show significant variations across each site. Therefore, although the PM_{10} concentrations across four sites vary significantly, the contribution of both mineral dust and inorganic salts at each site were similar.

3.2. Trace Elements in PM_{10}

In contrast to the major metals (Na, K, Mg, Fe, and Al), the concentrations of many trace metals (Pb, Sr, Cu, Ni, As, Mn, Zn, V, Ba, and Mo) showed large variations among different sites. Most trace elements showed highest air concentrations at Rio Seco and lowest at Tingo Grande and Yarabamba (Table 1 and Figure 4), but the distribution pattern of each element was different. For example, the average air concentrations of Pb at Av. Independencia, Tingo Grande, and Yarabamba were 4.6 ± 1.0, 2.5 ± 0.5, and 2.0 ± 0.9 ng/m^3,

respectively, while Rio Seco averaged 51.1 ± 48.0 ng/m^3, an order of magnitude higher than the other three sites. In contrast, As concentrations among all the sites were similar. The average As concentrations at Rio Seco, Av. Independencia, Tingo Grande, and Yarabamba were 16.1 ± 5.8, 13.4 ± 2.4, 14.0 ± 2.3, and 12.7 ± 4.6 ng/m^3, respectively. The observed heterogeneity implied distinctive geochemical characteristics of the PM$_{10}$ across the four sites, suggesting the different trace elements likely originated from various sources located close to the sampling sites.

Table 1. Air concentration (in ng/m^3) of elements in each site. Highest mean concentrations are marked in bold font. The unit for trace elements (Pb-Mo) is ng/m^3 and for major elements (Fe-Ca) is μg/m^3.

Element	Rio Seco				Av. Independencia				Tingo Grande				Yarabamba			
	Min	Max	Mean	Stdev	Min	Max	Mean	Stdev	Min	Max	Mean	Stdev	Min	Max	Mean	Stdev
Pb	9.3	122.8	**51.1**	48.0	2.8	6.7	4.6	1.0	1.6	3.4	2.5	0.5	0.9	3.8	2.0	0.9
Sr	14.2	44.5	**27.0**	8.9	9.5	7.9	12.8	2.5	2.9	15.2	9.6	4.2	2.2	17.9	7.8	5.0
Cu	21.0	102.4	**51.3**	30.6	9.5	35.9	17.1	7.4	5.5	30.6	14.5	7.1	5.2	35.7	13.4	9.0
Ni	1.0	16.3	**3.5**	4.6	1.1	5.8	3.0	1.4	1.0	1.8	1.3	0.3	0.4	2.0	1.1	0.5
Ba	24.7	62.1	**36.6**	12.4	18.8	41.0	28.3	6.2	9.8	20.3	15.3	2.8	6.5	25.3	14.4	6.1
V	9.1	35.0	**19.6**	6.8	13.8	45.9	**21.3**	8.1	14.7	25.4	17.4	3.0	7.4	27.7	15.8	5.8
As	7.7	30.8	**16.1**	5.8	11.2	21.4	13.4	2.4	11.6	20.9	14.0	2.3	6.9	22.4	12.7	4.6
Zn	26.3	165.6	**63.6**	46.9	17.6	35.4	25.1	5.0	9.3	19.4	13.9	2.6	6.8	28.4	14.9	7.0
Mn	28.0	67.0	**41.6**	13.2	14.4	26.5	20.2	2.7	8.4	23.8	16.9	4.6	5.4	33.4	15.1	8.4
Mo	0.7	2.5	**1.3**	0.6	0.6	1.0	0.8	0.1	0.3	1.1	0.6	0.2	0.3	1.4	0.6	0.3
Fe	0.9	1.9	**1.3**	0.3	0.7	1.3	0.9	0.1	0.4	1.1	0.8	0.2	0.3	1.5	0.7	0.4
Na	1.0	3.5	**2.0**	0.7	1.1	2.5	1.7	0.4	0.8	2.1	1.4	0.4	0.7	2.3	1.3	0.5
K	0.4	0.9	**0.8**	0.2	0.4	0.7	0.5	0.1	0.2	0.9	0.6	0.2	0.1	0.9	0.4	0.2
Mg	0.4	0.7	**0.6**	0.1	0.3	0.6	0.4	0.1	0.3	0.5	0.4	0.1	0.1	0.7	0.3	0.2
Ca	1.3	2.9	**2.1**	0.6	1.1	1.7	1.3	0.2	0.6	1.6	1.1	0.3	0.4	1.9	0.9	0.5

The mass-weighted concentrations of trace elements (Table 2 and Figure 5) were used to investigate the geochemical characteristics of PM$_{10}$ samples at each site. Because of the significant variations in PM$_{10}$ levels among our sampling sites, the mass-weighted concentrations of the trace elements among the four sites (Figures 4 and 5) show different patterns from their air concentrations. Mass-weighted concentrations of Cu, Pb, and Sr were highest at Rio Seco, Ba and Ni were highest at Av. Independencia, and As and V were most enriched at Tingo Grande and Yarabamba. In the meantime, Mn and Mo displayed similar mass-weighted concentrations among all the sites. These variations among the sites support the hypothesis that each element may originate from distinctive sources. Therefore, we partition the potential sources of trace elements in PM$_{10}$ into dust/soil emissions and metal emissions. Dust/soil emissions represent the trace metals that exist in the dust/soil particles and metal emissions include direct metal emissions (e.g., V emission during fossil fuel combustion) and metal-rich particle emissions (e.g., processing Cu-rich minerals). Since the sites are not far from each other, the contribution of mineral dust and inorganic salts should be similar among all the sites, and the mass-weighted concentrations of an element from dust/soil emissions should be the same among all the sites. In contrast, direct metal emissions could increase the amount of an element in the PM$_{10}$ without significantly impacting the total PM$_{10}$ level in the air, resulting in different mass-weighted concentrations among all the sites.

We used both the observed air and mass-weighted concentrations to estimate the relative contribution of dust/soil emissions and metal emissions to each element. The mass concentrations of Mn and Mo are homogeneous among the sites, and their concentrations can be attributed to the regional background. We suggest these elements were mainly from dust/soil emissions or "background PM" and the contributions of these metals by metal emissions were minimal. The remaining elements (Pb, Sr, Cu, Ba, Ni, V, and As) showed different mass-weight concentrations among each site, suggesting local metal emissions were important sources for these elements. In the following discussion we will separately discuss the metal emission contribution of each metal, and their potential sources.
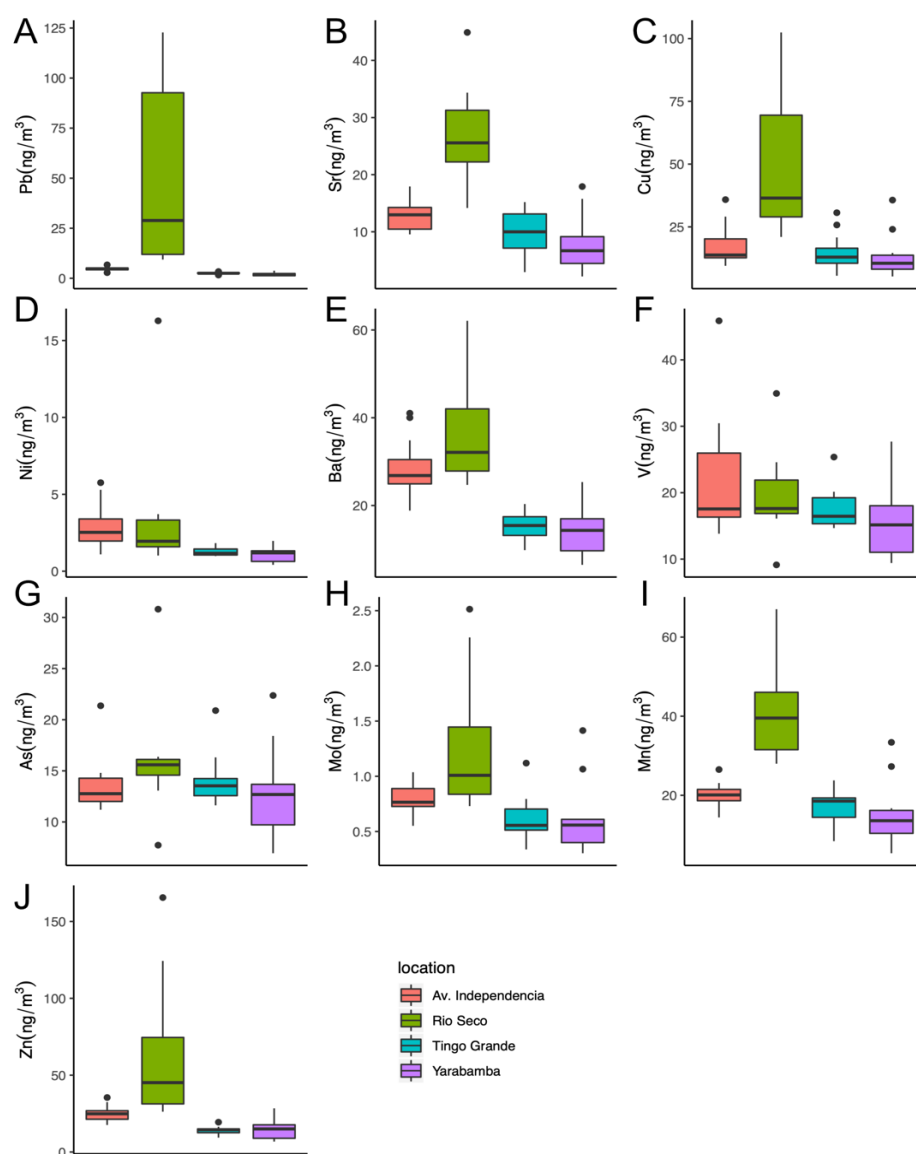
Figure 4. Box plot of the air concentrations (in ng/m^3) of trace elements at each site.

Table 2. Mass-weighted concentration of elements in PM$_{10}$ in each site. Highest mean concentrations are marked in bold font. The unit for trace elements (Pb-Mo) is ppm and for major elements (Fe-Ca) is %.

| Element	Rio Seco				Av. Independencia				Tingo Grande				Yarabamba			
	Min	Max	Mean	Stdev	Min	Max	Mean	Stdev	Min	Max	Mean	Stdev	Min	Max	Mean	Stdev
Pb	71	682	**277**	256	30	67	46	9	22	67	34	13	17	77	37	20
Sr	77	237	**157**	47	86	171	127	24	46	264	122	58	60	276	134	70
Cu	117	551	**293**	155	105	322	170	69	77	320	187	80	97	425	230	105
Ni	4	88	21	25	12	66	**30**	15	10	39	17	8	9	46	21	12
Ba	108	323	213	62	198	401	**281**	55	131	431	211	93	161	583	273	159
V	40	212	121	56	130	412	211	76	131	460	248	117	182	600	**297**	140
As	34	172	97	39	97	192	134	24	104	384	197	89	137	514	**240**	120
Zn	137	920	**362**	251	191	418	250	55	119	434	195	99	126	646	282	175
Mn	123	373	245	80	157	304	203	36	140	443	225	93	139	550	**271**	142
Mo	3	14	8	4	7	12	8	2	4	16	8	3	6	23	**11**	5
Fe	0.4	1.1	0.8	0.2	0.8	1.3	0.9	0.1	0.6	2.0	1.0	0.4	0.7	2.6	**1.3**	0.7
Na	0.5	2.0	1.2	0.5	1.2	2.1	1.6	0.3	1.1	3.5	1.9	0.6	1.5	5.0	**2.4**	1.1
K	0.2	0.6	0.4	0.1	0.4	0.7	0.5	0.1	0.4	1.7	**0.8**	0.4	0.4	1.6	0.7	0.4
Mg	0.2	0.4	0.3	0.1	0.3	0.5	0.4	0.1	0.4	0.9	0.5	0.2	0.3	1.1	**0.6**	0.3
Ca	0.7	1.6	1.2	0.3	1.1	1.7	1.3	0.2	0.9	3.0	1.5	0.6	1.0	3.3	**1.7**	0.8
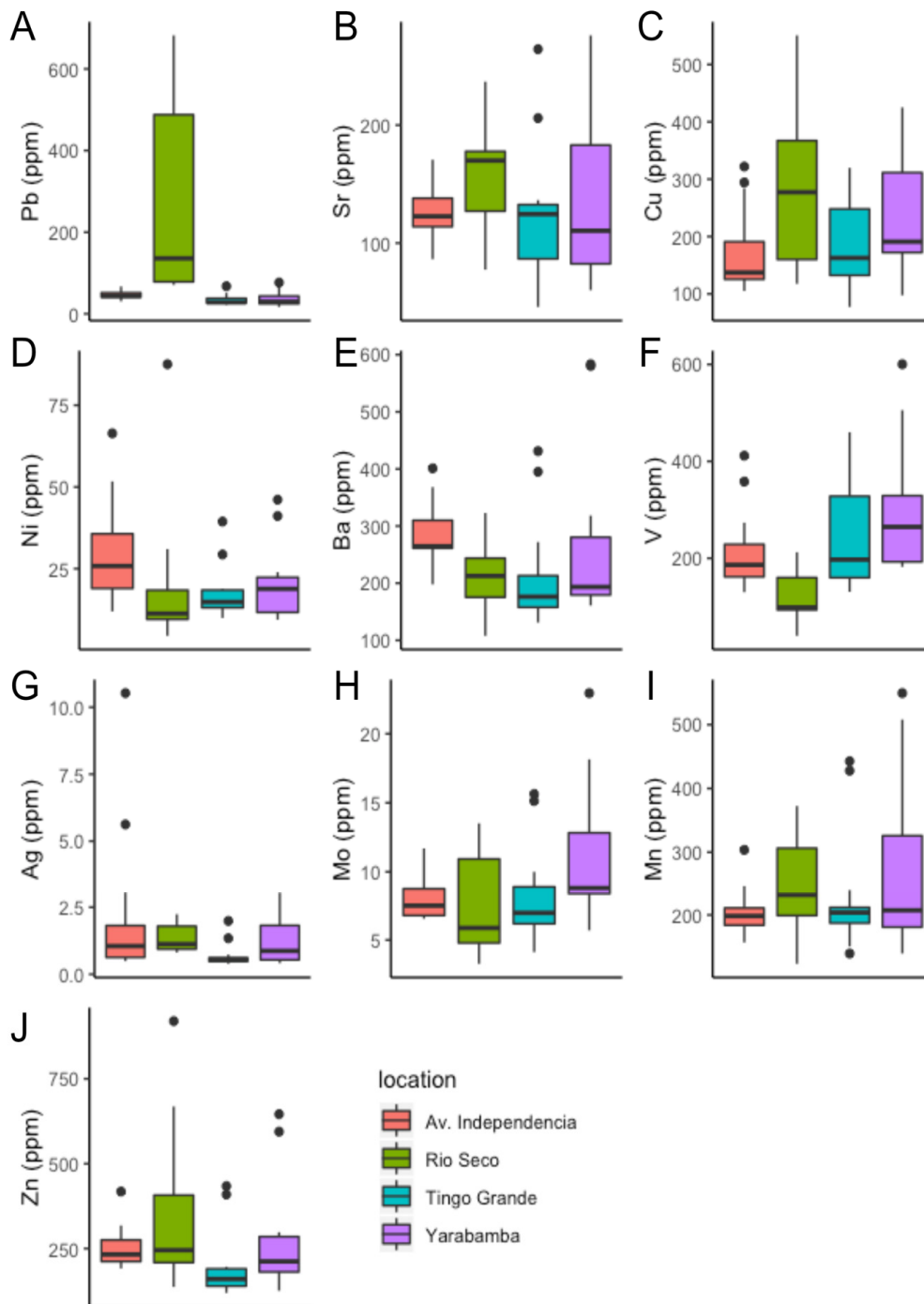
Figure 5. Box plot of mass-weighted concentrations (in ppm) of trace elements in the PM_{10} at each site.

3.3. Metal Emissions for Pb, Cu, Sr, Ba, Ni, V, and As

PM_{10} Pb was very high at Rio Seco, and we suggest that it originated from the local industrial activities. The mean air concentration of Pb at Rio Seco was 51 ng/m^3, 11 to 25 times higher than the other sites (2.0 to 4.6 ng/m^3), and the average mass concentration of 277 ppm was also an order of magnitude higher than the other sites (34–46 ppm). The Pb air concentrations at Rio Seco were similar to those observed at some heavily industrialized areas in Peru, such as Huancayo, in which 24–153 ng/m^3 Pb were observed [33]. The elevated concentration and the strong variations of Pb concentrations among the four sites suggest the Pb at Rio Seco could be almost entirely originated from local emissions. Similar enrichment in Pb is also observed in surface soils at Rio Seco [23], suggesting strong Pb

emission sources exist in this region. Coal combustion could contribute to the observed Pb enrichment. A previous study discovered elevated Pb concentrations in Peruvian coal, with 5–226 ppm Pb [34]. Since Rio Seco has heavy industrial activities, including tanneries, manufacturing plants, and brick kilns, most of which consume significant amounts of coal, the observed Pb in the PM_{10} likely originated from such activities. However, the deposition of large particles (>2.5 μm) is fast; therefore, the other sites (>15 km from Rio Seco) may not be significantly affected by the high Pb emissions in Rio Seco.

The elevated Cu concentrations in PM_{10} at all sites could possibly be linked to local dust and mining activities. Rio Seco has the highest mean mass-weighted concentration of 293 ppm, followed by Yarabamba (230 ppm), Tingo Grande (187 ppm), and Av. Independencia (170 ppm). The Cu at all four sites showed significant enrichment compared to other studies where desert dust was a major PM source. For example, the Cu mass concentration in Sahara dust [35] and dust from the Taklamakan Desert, China [36] was in the range 20–100 ppm, significantly lower than the average Cu mass fraction in our sampling sites. These observed high Cu concentrations suggest there was significant Cu emission at Arequipa. If we assume the dust/soil particles contained 60 ppm Cu (average value of Sahara dust and dust from Taklimakan Desert), then the elevated Cu in our PM_{10} samples must have originated from local emissions, which accounted for 64–80% of Cu in the PM_{10}. The Cu emissions might originate from mining activities and industrial activities. Tingo Grande and Yarabamba sites were close to one of the largest open-pit Cu-Mo mines in the world [37]. The mine is located ~30 km southwest of Arequipa, ~10 km away from Tingo Grande and Yarabamba sites, ~20 km from Av. Independencia, and ~30 km from Rio Seco. The mine ore contains ~0.5% Cu [37], thus, as little as 1.4–1.9 ug/m^3 of Cu-enriched dust could account for 100% of the Cu at Tingo Grande and Yarabamba. Therefore, we suggest the mining activities were the source of the PM_{10} Cu at Tingo Grande and Yarabamba. The average Cu mass (293 ppm) at Rio Seco was significantly higher than the other sites despite Rio Seco being furthest from the mine, indicating an additional local Cu emission source near Rio Seco. These high aerosol Cu concentrations at Rio Seco possibly originated from the surrounding leather processing plants that use copper sulfate during the tanning process. This is consistent with previous studies showing that leather processing activities, especially tanneries, can introduce Cu into groundwater and surface soil [38]. Here we show that they can possibly lead to elevated Cu concentrations in PM_{10} as well.

The enrichment of Sr at Rio Seco, relative to the other sites, suggests some anthropogenic Sr emissions at Rio Seco. Both Sr concentrations and Sr/Ca ratios at Av. Independencia, Yarabamba, and Tingo Grande were similar (Figure 5). The average mass-weighted concentrations of Sr at Av. Independencia, Yarabamba, and Tingo Grande were 127 ± 24 ppm, 122 ± 58 ppm, and 134 ± 70 ppm, respectively. These values are similar to Sr concentrations observed in Sahara dust and the Taklamakan Desert [35,39] and many studies that have shown that Sr primarily originated from crustal materials, such as road dust, mineral dust, and topsoil [40,41]. Both are consistent with our hypothesis that earth metals in Arequipa PM_{10} mainly originated from regional dust/soil emissions. In addition, high PM_{10} Sr content was usually associated with high Ca and Mg content, two common alkaline earth elements [42]. Ca and Mg in the region are associated with surface minerals such as gypsum [29,43], which are ubiquitous in the Atacama Desert. Therefore, if Sr is mostly from dust, then Sr/Ca ratios should be invariant across the low pollution sites. This agrees with the observed Sr/Ca ratios at these sites of 0.010 ± 0.001, 0.008 ± 0.001, and 0.008 ± 0.002 at Av. Independencia, Yarabamba, and Tingo Grande, respectively. In contrast, the Sr/Ca ratios at Rio Seco were 0.013 ± 0.002, 30–60% higher than the other sites. Likewise, the averaged mass-weighted concentration of Sr in PM_{10} at Rio Seco was 157 ± 47 ppm, 20% higher than the other three sites, suggesting there is a slight enrichment of Sr at Rio Seco. Therefore, we suggest there was an additional Sr emission source at Rio Seco. This Sr source might be associated with the industrial activities at Rio Seco; however, the emission factors of Sr in different emission sources is unknown, and we suggest future studies could be conducted to investigate the origins of the Sr.

Ba in PM$_{10}$ showed enrichment at the Av. Independencia site and could be due to traffic emissions, which are higher at this site relative to the others. Similar to the other earth metals, a fraction of PM$_{10}$ Ba could also originate from other crustal material, which is consistent with the observed overall mass concentrations (>200 ppm) across the four sampling sites (Table 2). The average Ba mass concentrations at Rio Seco and Tingo Grande were 210 and 212 ppm, respectively, and 273 ppm at Yarabamba. The higher average concentration at Yarabamba was due to two outliers with extreme high concentrations (~580 ppm). If the outliers were excluded (Figure 5), the average Ba concentration at Yarabamba was also similar to Rio Seco and Tingo Grande (200 ± 20 ppm). Since these sites showed overall consistent Ba mass-weight concentrations, we speculate the Ba in these sites was primarily sourced from dust/soil emissions. In contrast, Av. Independencia had an average Ba concentration of 281 ppm, 80 ppm higher than the rest of the sites. The elevated concentration might suggest the existence of Ba emission sources near the Av. Independencia site. The Av. Independencia site is in the city center (Figure 1) and close to commercial areas and residential neighborhoods; therefore, the elevated concentrations of these elements suggest significant contributions from residential emissions in such an urban environment. It is also an area with heavy traffic and high mobile emissions [24] and particles produced during the wearing of vehicle brake pads are a potential local source of Ba enrichment. Braking pads use BaSO$_4$ to increase their density and lifetime and particles emitted during vehicle braking displayed high Ba concentrations [44], especially heavy-duty vehicles that produce PM$_{10}$ containing >880 ppm Ba [45]. Therefore, it is possible that the heavy traffic near the Av. Independencia might be responsible for the elevated Ba concentrations. This is supported by the slightly elevated Cu concentration at Av. Independencia. Previous work [45] showed that the emission factors of Cu and Zn from traffic are similar to that of Ba. Although the PM$_{10}$ Cu concentrations at Av. Independencia were lower than other sites that have strong Cu emission sources, these observed concentrations were still significantly higher than the Cu mass concentration in pristine Sahara dust [35] and dust from the Taklamakan Desert, China [36]. Therefore, we suggest the traffic emissions might also contribute to the Cu observed at Av. Independencia. In contrast, elevated Zn concentrations in PM$_{10}$ were not observed at Av. Independencia. The PM$_{10}$ Zn concentrations at all the sites were similar to the Zn concentrations of pristine mineral dust; therefore, we suggest future work is needed to better constrain the metal emissions from traffic activities at Arequipa.

The elevated Ni concentration at Av. Independencia supports the hypothesis that emissions from diesel and gasoline combustion contribute more PM$_{10}$ relative to Rio Seco, Tingo Grande, and Yarabamba. The mass concentration of Ni at Av. Independencia was 30 ppm, ~50% higher than the other three sites (21 ppm, 17 ppm, and 21 ppm at Rio Seco, Tingo Grande, and Yarabamba, respectively). Previous studies have linked the aerosol Ni component with combustions of coal, crude oil, diesel, and gasoline [44,46–48]. Since Av. Independencia is located in an area with heavy traffic and high mobile emissions [24], we suggest the Ni in our PM$_{10}$ samples may have originated from vehicle emissions. Previous studies show high Ni concentrations in PM near roads. PM samples collected from four industrial sites in South Korea showed average Ni concentrations in the range 40–60 ppm [46], which is similar to our samples (30 ± 15 ppm), supporting our hypothesis that the Ni was primarily sourced from vehicle emissions. This is consistent with the observed high aerosol Ba concentrations at Av. Independencia, indicating that both Ba and Ni emissions were probably also sourced from vehicle emissions.

The V in PM$_{10}$ was likely originated from fossil fuel combustion. The averaged air concentration of V at Arequipa was 19 ng/m^3, 38 times higher than the measured values at Santiago, Chile [49], which showed an average V concentration of 0.5 ng/m^3, suggesting even stronger local V emissions in Arequipa. Previous studies have suggested that during fossil fuel combustion, 69% of V contained in fossil fuel could be emitted into the atmosphere [50]; therefore, the fossil fuel combustion at our sampling sites should be an important V source. This was supported by the V/Ni ratios in the PM$_{10}$ samples.

Assuming fossil fuel combustion was the sole source of V and Ni in urban regions [51], the V/Ni ratios in PM_{10} should imprint the V/Ni ratios in the fossil fuel. The V/Ni ratios in our sampling sites ranged from 8.3 to 15.5, averaging at 11.7. The observed V/Ni ratios were in general agreement with the V/Ni ratios observed in fossil fuels worldwide, which are in the range 0–4 [52–56] and can be as high as 10–17 [57], suggesting both Ni and V were likely sourced from fossil fuel combustions. However, the V/Ni ratios in fossil fuel used in Arequipa were not determined; therefore, future work is needed to confirm the origin of Ni and V.

As showed a similar distribution pattern as V. The air concentrations of As averaged 16.1 ± 5.8, 13.4 ± 2.4, 14.0 ± 2.3, and 12.7 ± 4.6 ng/m^3 at Rio Seco, Av. Independencia, Tingo Grande, and Yarabamba, respectively. These values were higher than some urban or industrial regions, such as downtown Los Angeles [58] and Huelva, Spain [59], but were lower than heavily-polluted areas, such as Shanghai during the winter [60] and Taiyuan, China [61]. The similar air concentrations of As among all the sites may suggest ubiquitous As emissions in the entire region [62]. The emissions of airborne As was often associated with sulfur [63]; therefore, coal and other fossil fuel burning activities could be a major sources of airborne As [61,64]. Furthermore, As could appear naturally in the sulfur-bearing minerals (e.g., as arsenopyrite) or be absorbed onto the surface of oxides and clay minerals [65]. High As concentrations in this region are due to geologic factors resulting in As-rich volcanic bedrock and through weathering and lixiviation, and it is found in toxic concentrations in the atmosphere, soil, and water of the Atacama Desert [66]. Therefore, the open-pit mining activities near Tingo Grande and Yarabamba could have also contributed to the observed airborne As.

4. Conclusions

This work reported the concentrations of Pb, Sr, Cu, Ni, As, Mn, Zn, V, Ba, and Mo in the PM_{10} collected at four sites around Arequipa, Peru. The concentrations of major elements (Ca, K, Na, Mg, Al, and Fe) in the PM_{10} samples were similar across all the sites, suggesting that mineral dust was a major component of the PM_{10} at all the sites. However, the concentrations of trace elements varied significantly among different sites, suggesting that these elements were originated from a mixing of (1) trace metals in local soil/dust, and (2) metal emissions. The trace element data suggest that Mn and Mo in the PM_{10} were mainly originated from soil/dust; Pb, Ni, As, and V were most likely sourced from anthropogenic metal emissions; and Cu, Ba and Sr were originated from a combination of soil/dust and anthropogenic emissions. The industrial activities at Rio Seco contributed to significant Pb, Cu, and possibly Sr emissions, while the mining processes at the Tingo Grande and Yarabamba showed strong Cu emissions. Fossil fuel combustions produced significant Ni, V, and As emissions, and the elevated Ba concentration in the city of Arequipa was mainly from brake wear emissions with the heavy traffic in the city. Our study shows that air pollution, especially elevated levels of PM_{10} in Arequipa, should be of great concern due to the rapid urbanization in the region. In addition, our study implies that the origins of metals in PM_{10} are complex, consisting of both local soil/dust and anthropogenic emissions; therefore, emissions regulations are in dire need. Future research in this area should focus on investigating potential sources of toxic PM elements such as mines, industrial production plants, and areas with high vehicle traffic. Further, determining the contribution of vehicle emissions to other tracers is particularly warranted given the outdated information on vehicles in service in Arequipa.

References

1. Dockery, D.W.; Pope, C.A.; Xu, X.; Spengler, J.D.; Ware, J.H.; Fay, M.E.; Ferris, B.G., Jr.; Speizer, F.E. An association between air pollution and mortality in six US cities. *N. Engl. J. Med.* **1993**, *329*, 1753–1759. [CrossRef]
2. Wilson, A.M.; Salloway, J.C.; Wake, C.P.; Kelly, T. Air pollution and the demand for hospital services: A review. *Environ. Int.* **2004**, *30*, 1109–1118. [CrossRef] [PubMed]
3. Karar, K.; Gupta, A. Seasonal variations and chemical characterization of ambient PM10 at residential and industrial sites of an urban region of Kolkata (Calcutta), India. *Atmos. Res.* **2006**, *81*, 36–53. [CrossRef]
4. Künzli, N.; Mudway, I.S.; Götschi, T.; Shi, T.; Kelly, F.J.; Cook, S.; Burney, P.; Forsberg, B.; Gauderman, J.W.; Hazenkamp, M.E.; et al. Comparison of Oxidative Properties, Light Absorbance, and Total and Elemental Mass Concentration of Ambient PM2.5 Collected at 20 European Sites. *Environ. Health Perspect.* **2006**, *114*, 684–690. [CrossRef] [PubMed]
5. Hu, M.; Jia, L.; Wang, J.; Pan, Y. Spatial and temporal characteristics of particulate matter in Beijing, China using the Empirical Mode Decomposition method. *Sci. Total Environ.* **2013**, *458–460*, 70–80. [CrossRef] [PubMed]
6. Silva, J.; Rojas, J.; Norabuena, M.; Molina, C.; Toro, R.A.; Leiva-Guzmán, M.A. Particulate matter levels in a South American megacity: The metropolitan area of Lima-Callao, Peru. *Environ. Monit. Assess.* **2017**, *189*, 635. [CrossRef]
7. Duce, R.A.; Hoffman, G.L.; Zoller, W.H. Atmospheric Trace Metals at Remote Northern and Southern Hemisphere Sites: Pollution or Natural? *Science* **1975**, *187*, 59–61. [CrossRef]
8. Chow, J.C.; Watson, J.G.; Lowenthal, D.H.; Hackney, R.; Magliano, K.; Lehrman, D.; Smith, T. Temporal Variations of PM2.5, PM10, and Gaseous Precursors during the 1995 Integrated Monitoring Study in Central California. *J. Air Waste Manag. Assoc.* **1999**, *49*, 16–24. [CrossRef]
9. Rodríguez, S.; Querol, X.; Alastuey, A.; Viana, M.-M.; Alarcón, M.; Mantilla, E.; Ruiz, C. Comparative PM10–PM2.5 source contribution study at rural, urban and industrial sites during PM episodes in Eastern Spain. *Sci. Total. Environ.* **2004**, *328*, 95–113. [CrossRef]
10. Sweet, C.W.; Vermette, S.J.; Landsberger, S. Sources of toxic trace elements in urban air in Illinois. *Environ. Sci. Technol.* **1993**, *27*, 2502–2510. [CrossRef]
11. Al-Momani, I.F.; Daradkeh, A.; Haj-Hussein, A.T.; Yousef, Y.A.; Jaradat, Q.; Momani, K. Trace elements in daily collected aerosols in Al-Hashimya, central Jordan. *Atmos. Res.* **2005**, *73*, 87–100. [CrossRef]
12. D'Alessandro, A.; Lucarelli, F.; Mandò, P.; Marcazzan, G.; Nava, S.; Prati, P.; Valli, G.; Vecchi, R.; Zucchiatti, A. Hourly elemental composition and sources identification of fine and coarse PM10 particulate matter in four Italian towns. *J. Aerosol Sci.* **2003**, *34*, 243–259. [CrossRef]
13. Quiterio, S.L.; Da Silva, C.R.S.; Arbilla, G.; Escaleira, V. Metals in airborne particulate matter in the industrial district of Santa Cruz, Rio de Janeiro, in an annual period. *Atmos. Environ.* **2004**, *38*, 321–331. [CrossRef]
14. Tsai, Y.I.; Kuo, S.-C.; Lin, Y.-H. Temporal characteristics of inhalable mercury and arsenic aerosols in the urban atmosphere in southern Taiwan. *Atmos. Environ.* **2003**, *37*, 3401–3411. [CrossRef]
15. Nriagu, J.O.; Davidson, C.I. *Toxic Metals in the Atmosphere*; John Wiley & Sons: Hoboken, NJ, USA, 1986.
16. Manoli, E.; Voutsa, D.; Samara, C. Chemical characterization and source identification/apportionment of fine and coarse air particles in Thessaloniki, Greece. *Atmos. Environ.* **2002**, *36*, 949–961. [CrossRef]
17. Monaci, F.; Moni, F.; Lanciotti, E.; Grechi, D.; Bargagli, R. Biomonitoring of airborne metals in urban environments: New tracers of vehicle emission, in place of lead. *Environ. Pollut.* **2000**, *107*, 321–327. [CrossRef]
18. Moreno, T.; Oldroyd, A.; McDonald, I.; Gibbons, W. Preferential Fractionation of Trace Metals–Metalloids into PM10 Resuspended from Contaminated Gold Mine Tailings at Rodalquilar, Spain. *Water Air Soil Pollut.* **2006**, *179*, 93–105. [CrossRef]
19. Aneja, V.P.; Isherwood, A.; Morgan, P. Characterization of particulate matter (PM10) related to surface coal mining operations in Appalachia. *Atmos. Environ.* **2012**, *54*, 496–501. [CrossRef]
20. Romero, Y.; Diaz, C.; Meldrum, I.; Velasquez, R.A.; Noel, J. Temporal and spatial analysis of traffic—Related pollutant under the influence of the seasonality and meteorological variables over an urban city in Peru. *Heliyon* **2020**, *6*, e04029. [CrossRef]
21. Valdivia, A.E.L.; Larico, J.A.R.; Peña, J.S.; Wannaz, E.D. Health risk assessment of polycyclic aromatic hydrocarbons (PAHs) adsorbed in PM2.5 and PM10 in a region of Arequipa, Peru. *Environ. Sci. Pollut. Res.* **2019**, *27*, 3065–3075. [CrossRef]

22. U.S. EPA. *IO Compendium Method IO-3.5: Compendium of Methods for the Determination of Inorganic Compounds in Ambient Air: Determination of Metals in Ambient Particulate Matter Using Inductively Coupled Plasma/Mass Spectrometry (ICP/MS)*; EPA/625/R-96/010a; U.S. EPA: Cincinnati, OH, USA, 1999.

23. MINAM. *Informe Nacional de la Calidad de Aire 2013–2014*; MINAM: Lima, Peru, 2014.

24. INSIDEO S.A.C. *Informe de Monitoreo Ambiental Participativo de Calidad de Aire Distrito Uchumayo*; INSIDEO S.A.C.: Lima, Peru, 2014.

25. Karydis, V.A.; Tsimpidi, A.P.; Pozzer, A.; Astitha, M.; Lelieveld, J. Effects of mineral dust on global atmospheric nitrate concentrations. *Atmos. Chem. Phys. Discuss.* **2016**, *16*, 1491–1509. [CrossRef]

26. Prospero, J.M.; Olmez, I.; Ames, M. Al and Fe in PM 2.5 and PM 10 Suspended Particles in South-Central Florida: The Impact of the Long Range Transport of African Mineral Dust. *Water Air Soil Pollut.* **2001**, *125*, 291–317. [CrossRef]

27. Zhu, X.R.; Prospero, J.M.; Millero, F.J. Diel variability of soluble Fe(II) and soluble total Fe in North African dust in the trade winds at Barbados. *J. Geophys. Res. Space Phys.* **1997**, *102*, 21297–21305. [CrossRef]

28. Lafon, S.; Sokolik, I.N.; Rajot, J.L.; Caquineau, S.; Gaudichet, A. Characterization of iron oxides in mineral dust aerosols: Implications for light absorption. *J. Geophys. Res. Space Phys.* **2006**, *111*. [CrossRef]

29. Li, J.; Wang, F.; Michalski, G.; Wilkins, B. Atmospheric deposition across the Atacama Desert, Chile: Compositions, source distributions, and interannual comparisons. *Chem. Geol.* **2019**, *525*, 435–446. [CrossRef]

30. Olson, E.J.; Michalski, G.; Welp, L.R.; Larrea Valdivia, A.; Reyes, J.; Mamani, A.E., Sr.; Salcedo Pena, J.M.; Magara-Gomez, K.T.; Li, J.; Palma Arhuire, Y.E., Sr. Sulfur Isotope Constraints on PM2.5 Sulfate Aerosol Sources in Arequipa, Peru. *AGU Fall Meet. Abstr.* **2019**, *2019*, A23K-2926.

31. Valdivia-Silva, J.; Ortega, F. Mineralogical study of the hyper-arid Mars like-soils from Pampas de La Joya, southern Peru and its implications in the geochemistry of dry environments. *EPSC-DPS Jt. Meet.* **2011**, *2011*, 1798.

32. Valdivia-Silva, J.E.; Navarro-González, R.; Ortega-Gutierrez, F.; Fletcher, L.E.; Perez-Montaño, S.; Apaza, R.M.C.; McKay, C.P. Multidisciplinary approach of the hyperarid desert of Pampas de La Joya in southern Peru as a new Mars-like soil analog. *Geochim. Cosmochim. Acta* **2011**, *75*, 1975–1991. [CrossRef]

33. De La Cruz, A.H.; Roca, Y.B.; Suarez-Salas, L.; Pomalaya, J.; Tolentino, D.A.; Gioda, A. Chemical Characterization of PM2.5 at Rural and Urban Sites around the Metropolitan Area of Huancayo (Central Andes of Peru). *Atmosphere* **2019**, *10*, 21. [CrossRef]

34. Somoano, M.M.D.; Kylander, M.E.; López-Antón, M.A.; Suárez-Ruiz, I.; Tarazona, M.R.M.; Ferrat, M.; Kober, B.; Weiss, D.J. Stable Lead Isotope Compositions In Selected Coals From Around The World And Implications For Present Day Aerosol Source Tracing. *Environ. Sci. Technol.* **2009**, *43*, 1078–1085. [CrossRef]

35. Bozlaker, A.; Prospero, J.M.; Price, J.; Chellam, S. Linking Barbados Mineral Dust Aerosols to North African Sources Using Elemental Composition and Radiogenic Sr, Nd, and Pb Isotope Signatures. *J. Geophys. Res. Atmos.* **2018**, *123*, 1384–1400. [CrossRef]

36. Dong, S.; Weiss, D.J.; Strekopytov, S.; Kreissig, K.; Sun, Y.; Baker, A.R.; Formenti, P. Stable isotope ratio measurements of Cu and Zn in mineral dust (bulk and size fractions) from the Taklimakan Desert and the Sahel and in aerosols from the eastern tropical North Atlantic Ocean. *Talanta* **2013**, *114*, 103–109. [CrossRef] [PubMed]

37. Quang, C.X.; Clark, A.H.; Lee, J.K.W.; Guillén, J. 40Ar-39Ar ages of hypogene and supergene mineralization in the Cerro Verde-Santa Rosa porphyry Cu-Mo cluster, Arequipa, Peru. *Econ. Geol.* **2003**, *98*, 1683–1696. [CrossRef]

38. Haroun, M.; Idris, A.; Omar, S.S. A study of heavy metals and their fate in the composting of tannery sludge. *Waste Manag.* **2007**, *27*, 1541–1550. [CrossRef] [PubMed]

39. Jiang, Q.; Yang, X. Sedimentological and Geochemical Composition of Aeolian Sediments in the Taklamakan Desert: Implications for Provenance and Sediment Supply Mechanisms. *J. Geophys. Res. Earth Surf.* **2019**, *124*, 1217–1237. [CrossRef]

40. Bencharif-Madani, F.; Ali-Khodja, H.; Kemmouche, A.; Terrouche, A.; Lokorai, K.; Naidja, L.; Bouziane, M. Mass concentrations, seasonal variations, chemical compositions and element sources of PM10 at an urban site in Constantine, northeast Algeria. *J. Geochem. Explor.* **2019**, *206*, 106356. [CrossRef]

41. Galindo, N.; Yubero, E.; Nicolás, J.; Varea, M.; Crespo, J. Characterization of metals in PM1 and PM10 and health risk evaluation at an urban site in the western Mediterranean. *Chemosphere* **2018**, *201*, 243–250. [CrossRef]

42. White, W.H.; Hyslop, N.P.; Trzepla, K.; Yatkin, S.; Rarig, R.S., Jr.; Gill, T.E.; Jin, L. Regional transport of a chemically distinctive dust: Gypsum from White Sands, New Mexico (USA). *Aeolian Res.* **2015**, *16*, 1–10. [CrossRef]

43. Rech, J.; Quade, J.; Hart, W.S. Isotopic evidence for the source of Ca and S in soil gypsum, anhydrite and calcite in the Atacama Desert, Chile. *Geochim. Cosmochim. Acta* **2003**, *67*, 575–586. [CrossRef]

44. Manno, E.; Varrica, D.; Dongarrà, G. Metal distribution in road dust samples collected in an urban area close to a petrochemical plant at Gela, Sicily. *Atmos. Environ.* **2006**, *40*, 5929–5941. [CrossRef]

45. Sternbeck, J.; Sjödin, Å.; Andréasson, K. Metal emissions from road traffic and the influence of resuspension—Results from two tunnel studies. *Atmos. Environ.* **2002**, *36*, 4735–4744. [CrossRef]

46. Duong, T.T.; Lee, B.-K. Partitioning and mobility behavior of metals in road dusts from national-scale industrial areas in Korea. *Atmos. Environ.* **2009**, *43*, 3502–3509. [CrossRef]

47. Kong, S.; Lu, B.; Ji, Y.; Zhao, X.; Chen, L.; Li, Z.; Han, B.; Bai, Z. Levels, risk assessment and sources of PM10 fraction heavy metals in four types dust from a coal-based city. *Microchem. J.* **2011**, *98*, 280–290. [CrossRef]

48. Xu, H.; Ho, S.S.H.; Cao, J.; Guinot, B.; Kan, H.; Shen, Z.; Ho, K.F.; Liu, S.; Zhao, Z.; Li, J.; et al. A 10-year observation of PM2.5-bound nickel in Xi'an, China: Effects of source control on its trend and associated health risks. *Sci. Rep.* **2017**, *7*, 41132. [CrossRef] [PubMed]

49. Valdés, A.; Polvé, M.; Munoz, M.; Toutain, J.P.; Morata, D. Geochemical features of aerosols in Santiago de Chile from time series analysis. *Environ. Earth Sci.* **2013**, *69*, 2073–2090. [CrossRef]

50. Monakhov, I.N.; Khromov, S.V.; Chernousov, P.I.; Yusfin, Y.S. The Flow of Vanadium-Bearing Materials in Industry. *Metallurgist* **2004**, *48*, 381–385. [CrossRef]

51. Pandolfi, M.; Gonzalez-Castanedo, Y.; Alastuey, A.; De La Rosa, J.D.; Mantilla, E.; De La Campa, A.S.; Querol, X.; Pey, J.; Amato, F.; Moreno, T. Source apportionment of PM10 and PM2.5 at multiple sites in the strait of Gibraltar by PMF: Impact of shipping emissions. *Environ. Sci. Pollut. Res.* **2011**, *18*, 260–269. [CrossRef] [PubMed]

52. Ali, M.F.; Bukhari, A.; Saleem, M. Trace metals in crude oils from Saudi Arabia. *Ind. Eng. Chem. Prod. Res. Dev.* **1983**, *22*, 691–694. [CrossRef]

53. Amato, F.; Pandolfi, M.; Viana, M.; Querol, X.; Alastuey, A.; Moreno, T. Spatial and chemical patterns of PM10 in road dust deposited in urban environment. *Atmos. Environ.* **2009**, *43*, 1650–1659. [CrossRef]

54. Chow, J.C.; Watson, J.G.; Ashbaugh, L.L.; Magliano, K.L. Similarities and differences in PM10 chemical source profiles for geological dust from the San Joaquin Valley, California. *Atmos. Environ.* **2003**, *37*, 1317–1340. [CrossRef]

55. Ho, K.; Lee, S.; Chow, J.C.; Watson, J.G. Characterization of PM10 and PM2.5 source profiles for fugitive dust in Hong Kong. *Atmos. Environ.* **2003**, *37*, 1023–1032. [CrossRef]

56. Vega, E.; Mugica, V.; Reyes, E.; Sánchez, G.; Chow, J.; Watson, J. Chemical composition of fugitive dust emitters in Mexico City. *Atmos. Environ.* **2001**, *35*, 4033–4039. [CrossRef]

57. López, L.; Mónaco, S.L.; Galarraga, F.; Lira, A.; Cruz, C. VNi ratio in maltene and asphaltene fractions of crude oils from the west Venezuelan basin: Correlation studies. *Chem. Geol.* **1995**, *119*, 255–262. [CrossRef]

58. Chow, J.C.; Watson, J.G.; Fujita, E.M.; Lu, Z.; Lawson, D.R.; Ashbaugh, L.L. Temporal and spatial variations of PM2.5 and PM10 aerosol in the Southern California air quality study. *Atmos. Environ.* **1994**, *28*, 2061–2080. [CrossRef]

59. Sánchez-Rodas, D.; De La Campa, S.; De La Rosa, J.D.; Oliveira, V.; Gómez-Ariza, J.L.; Querol, X.; Alastuey, A. Arsenic speciation of atmospheric particulate matter (PM10) in an industrialised urban site in southwestern Spain. *Chemosphere* **2007**, *66*, 1485–1493. [CrossRef]

60. Zheng, J.; Tan, M.; Shibata, Y.; Tanaka, A.; Li, Y.; Zhang, G.; Zhang, Y.; Shan, Z. Characteristics of lead isotope ratios and elemental concentrations in PM10 fraction of airborne particulate matter in Shanghai after the phase-out of leaded gasoline. *Atmos. Environ.* **2004**, *38*, 1191–1200. [CrossRef]

61. Xie, R.; Seip, H.M.; Wibetoe, G.; Nori, S.; McLeod, C.W. Heavy coal combustion as the dominant source of particulate pollution in Taiyuan, China, corroborated by high concentrations of arsenic and selenium in PM10. *Sci. Total Environ.* **2006**, *370*, 409–415. [CrossRef]

62. Lu, H.; Chen, H.; Li, W.; Li, B. Transformation of arsenic in Yima coal during fluidized-bed pyrolysis. *Fuel* **2004**, *83*, 645–650. [CrossRef]

63. Zhao, C.; Luo, K. Sulfur, arsenic, fluorine and mercury emissions resulting from coal-washing byproducts: A critical component of China's emission inventory. *Atmos. Environ.* **2017**, *152*, 270–278. [CrossRef]

64. Kavouras, I.G.; Koutrakis, P.; Cereceda-Balic, F.; Oyola, P. Source Apportionment of PM10 and PM25 in Five Chilean Cities Using Factor Analysis. *J. Air Waste Manag. Assoc.* **2001**, *51*, 451–464. [CrossRef]

65. Goldberg, S. Competitive adsorption of arsenate and arsenite on oxides and clay minerals. *Soil Sci. Soc. Am. J.* **2002**, *66*, 413–421. [CrossRef]

66. Escalante, G.; Campos, V.L.; Valenzuela, C.; Yañez, J.; Zaror, C.; Mondaca, M.A. Arsenic resistant bacteria isolated from arsenic contaminated river in the Atacama Desert (Chile). *Bull. Environ. Contam. Toxicol.* **2009**, *83*, 657–661. [CrossRef] [PubMed]